Arabian Journal of Chemistry (2022) **15**, 104224

King Saud University

**Arabian Journal of Chemistry**

www.ksu.edu.sa
www.sciencedirect.com

ORIGINAL ARTICLE

# Removal of Pb(II) from water samples using surface modified core/shell CdZnS/ZnS QDs as adsorbents: Characterization, adsorption, kinetic and thermodynamic studies

**Kousar Yasmeen [a], Sadia Nawaz [a], Azhar Iqbal [a], Asma Siddiqui [a], Abdul Rehman Umar [b], Haji Muhammad [a,*], Maryam Shafique [c], Faheem Shah [d,*], Sobia Tahir [a], Abdul Majeed Khan [a], Muhammad Masab [e], Muddasir Hanif [f,*]**

[a] *Department of Chemistry, Federal Urdu University of Arts, Sciences and Technology, Gulshan-e-Iqbal Campus, Karachi 75300, Pakistan*
[b] *Institute of Supramolecular Science and Engineering (ISIS) - UMR 7006 University of Strasbourg CNRS, 8 All'ee Gaspard Monge, Strasbourg F-67000, France*
[c] *Department of Microbiology, Federal Urdu University of Arts, Sciences and Technology, Gulshan-e-Iqbal Campus, Karachi 75300, Pakistan*
[d] *Department of Chemistry, COMSATS University Islamabad, Abbottabad Campus, 22060 Abbottabad, Pakistan*
[e] *Department of Chemistry, Government Degree College Hangu, Hangu District, KPK, Pakistan*
[f] *Department of Chemistry and Chemical Engineering, Jiangxi Normal University, Nanchang, Jiangxi 330022, PR China*

Received 4 May 2022; accepted 29 August 2022
Available online 6 September 2022

**KEYWORDS**

Quantum dots;
Pb(II) ions;
CdZnS/ZnS;
Core/shell;
Multivariate analyses;
Adsorption

**Abstract** This research presents aqueous colloidal method to synthesize CdZnS/ZnS surface modified core/shell quantum dots (QDs) with capping agents 2-mercaptoacetic acid and 3-mercaptopropanoic acid. The QDs were characterized by the different analytical techniques. Using Plackett–Burman and Central composite designs, optimum conditions for the removal of Pb(II) from aqueous medium were developed: QDs (0.013 g) at pH 6.9, time of adsorption and desorption (20 min), temperature (61.1 °C) and dilution on 100 ppb standard solutions. Moreover, Freundlich models suggested that Pb(II) adsorption was favorable on the heterogeneous surface of QDs. The values of $\Delta G^{\circ}$ and $\Delta H^{\circ}$ (−59.26 KJ/mol.K) suggested the process was spontaneous and exothermic. The negative $\Delta S^{\circ}$ (−0.16 KJ/mol.K) indicates that the Pb(II) chemisorb on QDs. While, system

* Corresponding authors.
E-mail addresses: haji.muhammad@fuuast.edu.pk (H. Muhammad), shah_ceac@yahoo.com (F. Shah), muddasirhanif@yahoo.com (M. Hanif).
Peer review under responsibility of King Saud University.

Production and hosting by Elsevier

https://doi.org/10.1016/j.arabjc.2022.104224

follows the pseudo-second order rate equation which indicates that rate limiting step involves chemical reaction and could be influenced by the intraparticle/pore diffusion of Pb(II) ions with QDs. By using atomic absorption spectrophotometer, developed method was tested for Pb(II) removal from tap and ground water samples taken from the different districts of Karachi City. The % recovery for Pb(II) was found to be 96.4 % (tap water) and 94.8 % (ground water) with LOD = 0.1 ng $mL^{-1}$ and LOQ = 0.90 ng $mL^{-1}$.



## 1. Introduction

Heavy metal ions are harmful pollutants in industrial wastewater and common groundwater (Heidari-Chaleshtori and Nezamzadeh-Ejhieh, 2015). Lead ions Pb(II) are toxic and accumulate in the human body through drinking water (Sultanbayeva et al., 2013). Even very low dose of Pb ions entering in the human body for an extended period can cause health problems such as nausea, cancer, coma, convulsions, renal failure, and subtle effects on metabolism and intelligence (Staff and Organization, 1996). Thus, eradication of Pb(II) from water became an urgent problem for environmental safety throughout the world. Therefore for the removal of Pb(II) from water and wastewater, several physical and chemical technologies have been adopted including electrodialysis (Gurreri et al., 2020), flocculation-coagulation (Hargreaves et al., 2018a; Hargreaves et al., 2018) chemical precipitation (Chen et al., 2018), reverse osmosis (Thaçi and Gashi, 2019), filtration (Zhu et al., 2018), ion exchange (Murray and Örmeci, 2019), and adsorption (Wu et al., 2021). Among these techniques adsorption is simple, cost effective, regenerative and robust approach for the removal of pollutants from wastewater (Anari-Anaraki and Nezamzadeh-Ejhieh, 2015).

So far several traditional adsorbents such as tea waste (Amarasinghe and Williams, 2007), mineral (Prasad et al., 2008), CNTs-Fe oxide magnetic composites (Peng et al., 2005), activated carbon (Reed et al., 2000), kaolinite clay (Jiang et al., 2009) have been employed for Pb(II) removal from the aqueous mediums. Still there are some situations where small quantity of Pb(II) remains in water and waste water which causes harm to life (Okereafor et al., 2020). Therefore, researchers are still working hard to develop novel adsorbent materials with excellent removal efficiency while keeping these issues in mind.

Quantum dots (QDs) are semiconductor particles with three dimensions that are all restricted to the nanoscale (Alivisatos, 1996). At such small sizes (in close proximity to or smaller than the exciton Bohr radius), these nanostructured materials behave differently from bulk solids, because of quantum-confinement effects (Costa-Fernandez, 2006). As a result QDs have unique optical and electronic properties such as broad excitation spectra, narrow symmetric and tunable emission spectra between ultraviolet and infrared regions (Chan et al., 2002). Mostly, colloidal QDs with high photoluminescence quantum yields, photobleaching resistance, physic-chemical degradations, and excellent biocompatibility have proven to be unique optical materials in various applications, including cellular processes visualization (Ma et al., 2019) in vitro and in vivo imaging and labeling (Franke et al., 2016), luminescent sensors for chemical and biological species (Kazemifard et al., 2021) and targeted drug delivery. Currently, there are sensors available for detection of heavy metals ions which are based on electrochemical and colorimetric modeling of spectroscopy. Yet QDs has attracted more attention as sensitive and specific heavy metal ions probe high due to their versatile surface functionalization (Zou et al., 2015).

Therefore, in this research a colloidal method was used to synthesize the facile and inexpensive surface modified core/shell CdZnS/ZnS QDs in aqueous medium by using two different capping agents' 2-mercaptoacetic acid (2-MAA) and 3-mercaptopropanoic acid (3-MPA). The QDs were well characterized with the help of sophisticated techniques; XRD, SEM and EDS. Using Plackett–Burman and Central composite designs, optimum conditions for the removal of Pb (II) in aqueous medium were optimized. While atomic absorption spectroscopy was utilized to quantify the Pb(II) concentration in real water sample by QDs. Moreover, adsorption mechanism of Pb(II) on QDs was deeply evaluated through isotherm, thermodynamic and kinetic studies.

## 2. Experimental

### 2.1. Chemicals

Cadmium chloride ($CdCl_2{\cdot}2.5H_2O$, ≥98 %), zinc nitrate ($ZnNO_3{\cdot}6H_2O$, ≥98 %), sodium sulphide ($Na_2S{\cdot}9H_2O$, ≥ 99.9 %), sodium hydroxide (NaOH, ≥ 99 %), zinc chloride ($ZnCl_2$, ≥98 %), 2-mercaptoacetic acid (2-MAA, ≥ 98 %), ethanol and 3-mercaptopropionic acid (3-MPA, ≥98 %) purchased from Sigma Aldrich and were used without any distillation.

### 2.2. Synthesis of surface modified CdZnS (Core)/ZnS (Shell) QDs via different capping agents

Surface modified core/shell QDs were synthesized by following the reported aqueous colloidal method with modification (Yakoubi et al., 2016; Masab et al., 2018). Briefly, 0.0271 g of $CdCl_2{\cdot}2.5H_2O$ was dissolved in 50 mL of de-ionized water to form 2 mM solution. In similar manner the 1 mM solution of $ZnCl_2$ was prepared in a 50 mL by dissolving 0.0070 g in de-ionized water. 1 mM solution of 2-MAA was prepared in 100 mL de-ionized water by taking 71 µL with micropipette in a 100 mL in three-necked round bottom flask having 50 mL of de-ionized water. One by one 50 mL of each solution was added into the flask and nitrogen was purge for 15 min. Later flask was clasped on hotplate in a heating mantle with condenser and thermometer in two necks. After 10 min, stirred and heated mixture turns turbid which became clear when pH was adjustment to 8 with 2–2.5 mL of 1 M NaOH. After that prepared 10 mM solution of $Na_2S{\cdot}9H_2O$ by combining 0.1201 g in 50 mL de-ionized water was reckoned up into mixture solution. When solution attained temperature of 100 °C heating was stop and mixture was left on continuous stirring for approximately 3 h for growth of CdZnS QDs.

Meanwhile, in another beaker 1.1 mL of $Na_2S{\cdot}9H_2O$ (0.1 M) solution (5 mL de-ionize water by weighing of 0.1201 g), 1.1 mL of $ZnCl_2$ (0.15 M) solution (0.1022 g in 5 mL de-ionized water) and 2-MAA (50 µL from 0.04 M solution in 50 mL of de-ionized water) was taken. After few minutes, mixture turns turbid which became clear when pH was adjustment to 8 with 2–2.5 mL of 1 M NaOH. After 3 h, the mixture was injected into the crude solution of CdZnS QDs

after flux. The reaction was again heated for 1 h at 100 °C with constant stirring for development of CdZnS/ZnS core/shell QDs. After the completion of the process, 2.5 mL of ethanol was added into cooled reaction mixture for the removal of organic impurities through precipitation. For the elimination of inorganic impurities solid material was re-disperse into the solution, 15 mL of de-ionized water was poured and solution get centrifuge to form cluster. The centrifuged QDs were left in oven at 101 °C for 24 h. Likewise, QDs capped with 3MPA and CdZnS (core)/ZnS (shell) of same shape and structure were prepared by following aforementioned method using $ZnNO_3{\cdot}6H_2O$ instead of $ZnCl_2$ and 3MPA instead of 2-MAA.

### 2.3. Instrumentation

CdZnS/ZnS QDs dispersed in distilled water were initially characterized by UV–Visible spectra (Schimadzu, 1800 spectrophotometer) in 200–800 nm wavelength range, **S1**. The X-ray diffraction (XRD) patterns of QDs were recorded on Shimadzu XRD6000 system with Cu-Kα radiation (0.15406 nm). To study the functional groups involvement in the QDs synthesis FT-IR spectra were recorded with FT-IR Shimadzu 8400 s (S2 and ST1). For morphological analyses of QDs, scanning electron microscopy (SEM) (JSM-6380A, JEOL, Japan) and EDS (EX54175jMU, JEOL, Japan) images were taken. While, atomic absorption spectrophotometer (AAS) from PE-AAnalyst700 (Norwalk, CT, USA) was utilized for determination of Pb(II) in the water samples by QDs. All optical measurements were performed at room temperature and under ambient conditions.

### 2.4. Plackett–Burman design (PBD)

Two level PBD was carried out to distinguish the significant and insignificant variables and assess their mutual interaction as well as their effect on extraction efficacy. Minitab® 16.1.1 (Minitab Inc., State College, PA, USA) and STATISTICA 8 were used in this research model (design of experiments) which composed only on 24 experiments which is much lower than 64 ($2^6$) experiments for full factorial design. Pareto chart was plotted and confirmed the significance as well their effect on the efficiency of the extraction technique. Significant variables were identified as their bars in the said chart were passing beyond the vertical line ($t_{critical}$ value at $p \leq 0.05$) (Dilshad et al., 2021).

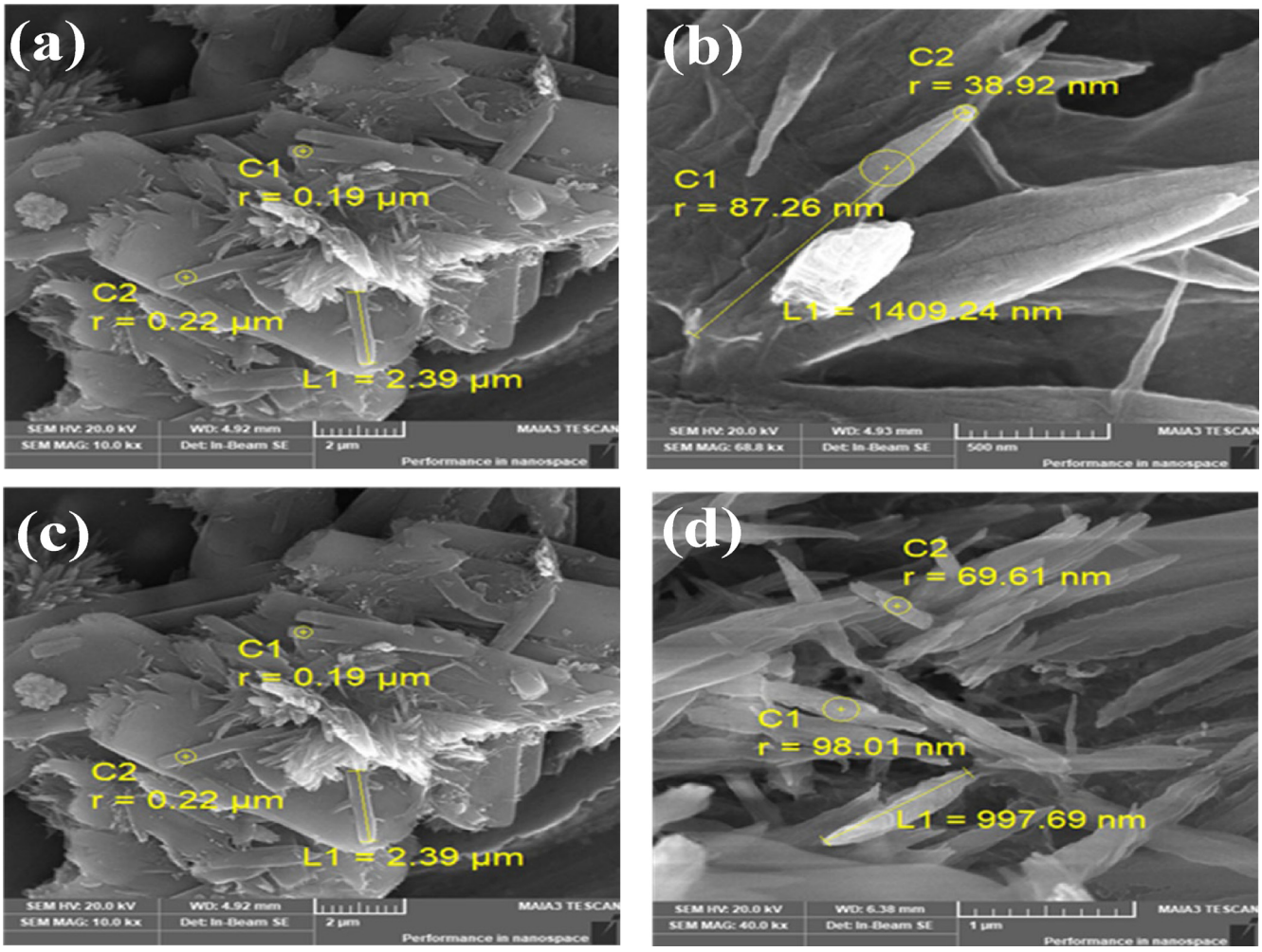


**Fig. 1** SEM Image of (a) CdZnS/ZnS@ 2-MAA QDs (using $ZnCl_2$ as salt), (b) CdZnS/ZnS@ 2-MAA QDs (using $ZnNO_3{\cdot}6H_2O$ as salt) & (c) CdZnS/ZnS@ 3-MPA QDs ($ZnCl_2$ salt) (d) CdZnS/ZnS@ 3- MPA QDs ($ZnNO_3{\cdot}6H_2O$ salt).

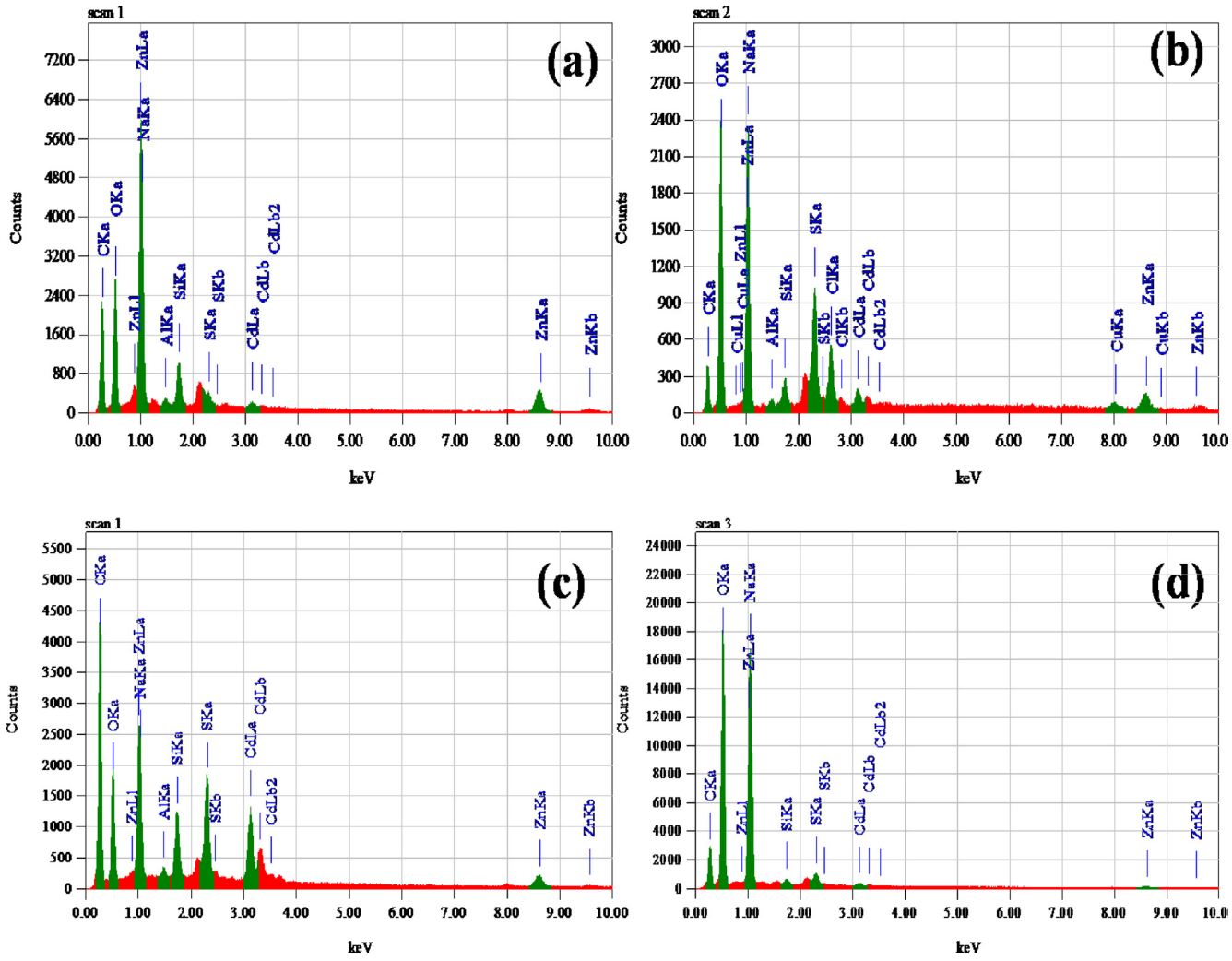


**Fig. 2** EDS Image of (a) CdZnS/ZnS@ 2-MAA QDs (using $ZnCl_2$ as salt), (b) CdZnS/ZnS@ 2-MAA QDs (using $ZnNO_3{\cdot}6H_2O$ as salt) (c) CdZnS/ZnS@ 3-MPA QDs ($ZnCl_2$ salt) (d) CdZnS/ZnS@ 3- MPA QDs ($ZnNO_3{\cdot}6H_2O$ salt).

### *2.5. Central composite design (CCD)*

Once the significant and insignificant variables were identified, the significant variables were considered for further optimization. Feasible values were assigned to the insignificant variables (assessed earlier through PBD) for further experiments. Significant variables were subjected to further optimization. In this multivariate optimization step, a central $2^{3+}$ star orthogonal composite design based on 26 experiments was performed to evaluate combined effect of these significant variables against % recoveries of analyte.

### *2.6. Removal of Pb(II) in batch experiments*

The removal of Pb(II) from the water samples using QDs was optimized under experimental parameters such as time, pH, temperature, adsorbent mass, and amount of Pb(II) for by the help of AAS, **S3**. In typical removal experiments, 0.01 g QDs were added into 0.001 g Pb(II) (or other subjected concentration) water sample and mixture was adjusted to optimized condition (**see ST2**) to get stirred for 24 h at ambient temperature. After centrifuging the suspensions, the Pb content of the supernatant was determined by the AAS and % removal was calculated using the following formula.

$$\%Removal = \frac{C_i - C_e}{C_i} \times 100$$

where, $C_i$ and $C_e$ are the initial and remaining concentration (ppm) of Pb(II) in water sample, respectively (Nawaz et al., 2020). Furthermore, AAS techniques was also used to quantify the presence and recovery of Pb(II) by QDs in real water samples by following same procedure with help of given formula.

$$\%Recovery = \frac{Extracted}{Added} \times 100$$

$$\%Recovery = \frac{SD}{Mean} \times 100$$

Moreover, averaged values from three runs of each experiment were presented.

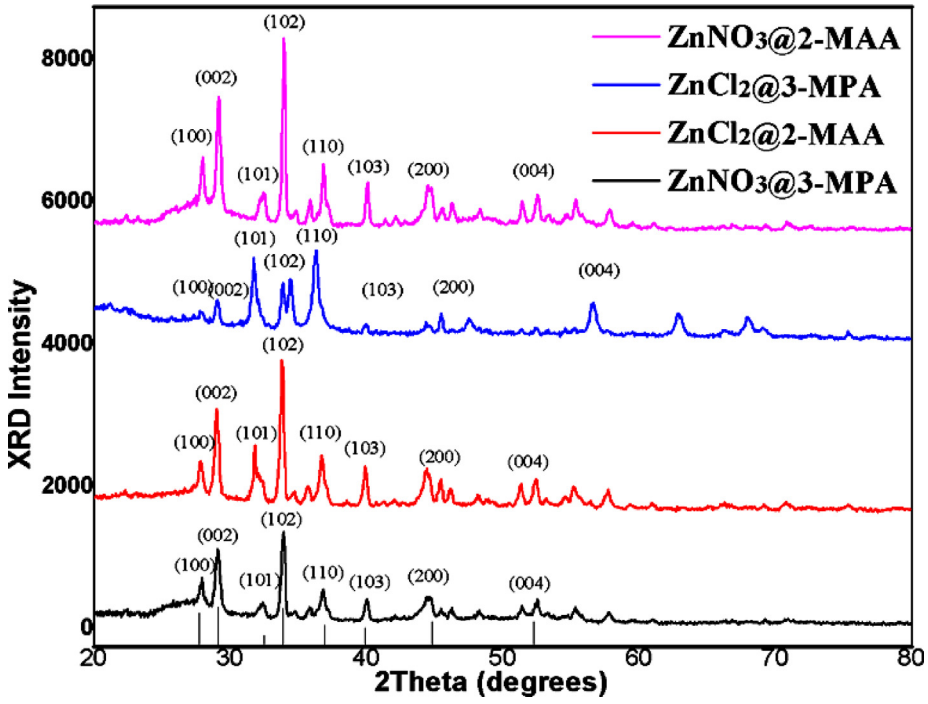


**Fig. 3** XRD motifs of CdZnS/ZnS QDs processed via divergent capping agents.

**Table 1** Factor and levels used in the factorial design.

| Variables | ID | Unit | Levels | | |
|---|---|---|---|---|---|
| | | | Lower | Higher | Optimum* |
| **pH** | A | – | 2 | 12 | 6.9 |
| **Temperature** | B | °C | 20 | 100† | 61.1 |
| **Adsorbent Amount** | C | g | 0.005 | 0.02 | 0.013 |
| **Time** | D | minutes | 5 | 20 | 15.3 |
| **Dilution** | E | mL | 100 | 500 | †† |

* Optimum values for significant factors.
† Practically used value is 85 °C as higher value.
†† Insignificant factors with convenient values.

## 3. Result and discussion

### 3.1. Structural characterization of CdZnS/ZnS QDs

The SEM images of surface modified CdZnS/ZnS QDs capped with 2-MAA and 3-MPA have signifies that core/shell QDs are crystalline in nature and their size in the range of quantum confinement effect. Fig. 1 (a, b) & (c, d) taken at low and high magnification levels showed the formation of variable nano-size QDs with strong compactness. The analysis of EDS Fig. 2(a, b) & (c, d) has also proved that prepared QDs contained Cd, Zn, S, O and C. The powder XRD spectrum of CdZnS/ZnS with 3-MPA and 2-MAA (Fig. 3) displayed eight peaks at $2\theta = 27.7°$, 29.1°, 32.4°,33.9°, 36.9°, 39.9°, 44.8°, 52.3° which are indexed to the (*hkl*) planes: (100), (002), (101), (102), (110), (103), (200), (004). These results verify that core/shell QDs have microscopic particle size and have nanocrystalline nature. Furthermore, the array of XRD peaks is present at those pure CdS and ZnS merge states, corresponding to the previously reported suppositions (Liu et al., 2013; Kumari and Kar, 2020). Debye-Scherer equation was also practiced for analysis of synthesized CdZnS/ZnS QDs crystallite size in which $D = 0.94\lambda/\beta \cos\theta$: where $\theta$ is the Bragg angle, $\beta$ is full circumference at half maximum and $\lambda$ is wavelength of the worn X-ray (1.5406 Å). The average crystallite size (D) from the planes of first peak is 16 nm.

### 3.2. Optimization of Pb(II) removal by multivariate study

Plackett–Burman design is known to be an efficient design, widely utilized as an optimization tool in method development. In contrast to traditional univariate optimization where only one variable is studied at one time, this design is more effective, prompt and easier design. Different experimental variable that

**Table 2a** Design matrix and the results of % R (n = 5).

| S. No. | A | B | C | D | E | % R |
|---|---|---|---|---|---|---|
| 1. | + | − | − | − | − | 65.2 ± |
| 2. | + | + | − | − | − | 32.3 ± |
| 3. | + | + | + | − | − | 45.1 ± |
| 4. | + | + | + | + | − | 61.0 ± |
| 5. | + | + | + | + | + | 27.8 ± |
| 6. | − | + | + | + | + | 70.7 ± |
| 7. | + | − | + | + | + | 29.3 ± |
| 8. | − | + | − | + | + | 59.5 ± |
| 9. | + | − | + | − | + | 24.1 ± |
| 10. | + | + | − | + | − | 39.7 ± |
| 11. | − | + | + | − | + | 42.1 ± |
| 12. | − | − | + | + | − | 77.5 ± |
| 13. | + | − | − | + | + | 49.5 ± |
| 14. | + | + | − | − | + | 18.0 ± |
| 15. | − | + | + | − | − | 45.0 ± |
| 16. | − | − | + | + | − | 65.7 ± |
| 17. | + | − | − | + | + | 21.1 ± |
| 18. | − | + | − | − | + | 23.8 ± |
| 19. | + | − | + | − | − | 47.1 ± |
| 20. | − | + | − | + | − | 36.0 ± |
| 21. | − | − | + | − | + | 40.5 ± |
| 22. | − | − | − | + | − | 69.4 ± |
| 23. | − | − | − | − | + | 43.4 ± |
| 24. | − | − | − | − | − | 66.2 ± |

**Table 2b** Central orthogonal composite design for the set of factors A, B, C and D (n = 6).

| S. No. | A | B | C | D | % R |
|---|---|---|---|---|---|
| 1. | $_{a}A^{o}$ | $_{a}B^{o}$ | $_{a}C^{o}$ | $_{a}D^{o}$ | 99.1 ± |
| 2. | − | − | − | − | 37.4 ± |
| 3. | + | − | − | − | 36.4 ± |
| 4. | − | + | − | − | 25.3 ± |
| 5. | + | + | − | − | 14.0 ± |
| 6. | − | − | + | − | 45.8 ± |
| 7. | + | − | + | − | 78.4 ± |
| 8. | − | + | + | − | 12.4 ± |
| 9. | + | + | + | − | 12.4 ± |
| 10. | − | − | − | + | 35.3 ± |
| 11. | + | − | − | + | 24.7 ± |
| 12. | − | + | − | + | 25.1 ± |
| 13. | + | + | − | + | 26.0 ± |
| 14. | − | − | + | + | 27.3 ± |
| 15. | + | − | + | + | 45.5 ± |
| 16. | − | + | + | + | 14.7 ± |
| 17. | + | + | + | + | 25.1 ± |
| 18. | $-A^{1}$ | $_{a}B^{o}$ | $_{a}C^{o}$ | $_{a}D^{o}$ | 2.3 ± |
| 19. | $+A^{2}$ | $_{a}B^{o}$ | $_{a}C^{o}$ | $_{a}D^{o}$ | 13.2 ± |
| 20. | $_{a}A^{o}$ | $-B^{1}$ | $_{a}C^{o}$ | $_{a}D^{o}$ | 9.8 ± |
| 21. | $_{a}A^{o}$ | $+B^{2}$ | $_{a}C^{o}$ | $_{a}D^{o}$ | 1.8 ± |
| 22. | $_{a}A^{o}$ | $_{a}B^{o}$ | $-C^{1}$ | $_{a}D^{o}$ | 11.3 ± |
| 23. | $_{a}A^{o}$ | $_{a}B^{o}$ | $+C^{2}$ | $_{a}D^{o}$ | 9.1 ± |
| 24. | $_{a}A^{o}$ | $_{a}B^{o}$ | $_{a}C^{o}$ | $-D^{1}$ | 4.6 ± |
| 25. | $_{a}A^{o}$ | $_{a}B^{o}$ | $_{a}C^{o}$ | $+D^{2}$ | 7.3 ± |
| 26. | $_{a}A^{o}$ | $_{a}B^{o}$ | $_{a}C^{o}$ | $_{a}D^{o}$ | 97.0 ± |

$-A^{1} = -3$, $+A^{2} = 17$, $_{a}A^{o} = 7$, $-B^{1} = -20$, $+B^{2} = 140$, $_{a}B^{o} = 60$, $-C^{1} = -0.0025$, $+C^{2} = 0.0275$, $_{a}C^{o} = 0.0125$, $-D^{1} = -5$, $+D^{2} = 35$, $_{a}D^{o} = 15$.

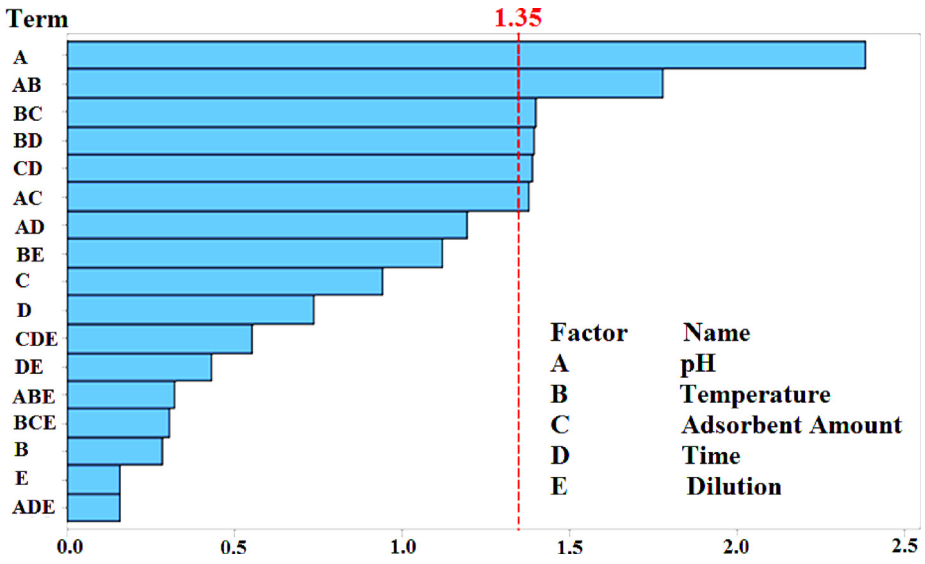


**Fig. 4** Pareto chart of the effects.

could possibly affect the efficacy of the proposed extraction technique were screened initially through PBD followed by CCD for optimization. These variables were pH, temperature, adsorbent amount, dilution, and adsorption/desorption time. Levels (higher and lower) of these variables along with their optimum values are shown in Table 1. Plackett–Burman matrix design with 24 experiment and the recoveries obtained are presented in Table 2a**.**

### *3.2.1. Central composite design (CCD)*

Significant variables, *i.e.*, pH, temperature, adsorbent amount, and adsorption/desorption time were further optimized through CCD. Any variation in the value of significant variables (from higher level to lower level and vice versa) influenced the % recoveries. This variation in % recoveries due to varying the levels of significant variable is depicted in Table 2b, and the same trend has been portrayed in the form of Pareto chart of the standardized effect (Fig. 4). Any variable bearing a $t_{critical}$ value greater than 1.350 (at the 95.0 % confidence interval) is termed as significant variable. The results obtained with CCD for significant variables are present in the Table 2b. The % recoveries of Pb(II) were found to be 1.8–99.1 %. At optimum values of these variables, maximum recovery of Pb(II) was achieved as shown in experiment no. 1 & 26. On the other hand, any deviation from the optimum value of any variable resulted in decrease of Pb(II) recovery (experiments no. 18–25 of Table 2b).

Results obtained with ANOVA are presented as **S3**, which were utilized in the order to validate the observed quadratic model at 95 % confidence level. To assess the significance of the proposed model for the efficiency of Pb(II) removal; a comparison of F-values was made, where $F_{calculated}$ (2.65) was found greater than $F_{critical}$ (2.42). Beside F-values, the same scenario was observed with p-value which was $< 0.0001$ (al Sadat Shafiof and Nezamzadeh-Ejhieh, 2020). Similarly, the lack-of-fit p-value $0.606 > 0.05$ and $F_{calculated} = 0.84 < F_{critical} = 2.93$ confirmed that it is insignificant, which means that this model can the fit the data appropriately.

The Fig. 5(a-d) showed the predicted response surface data obtained for various variables A/B, B/C, A/C and C/D against % recoveries of Pb(II). Once the 3D plots of response surface were plotted, quadratic equation for each pair of variables was obtained. The obtained quadratic equations for all these pairs of variables are given (Eqs. (1.1)–(1.4)).

$$\%Recovery\frac{A}{B} = 12.27 + 4.10x + 0.55y - 0.29x^2 - 1.19 \times 10^{-2}xy - 4.60 \times 10^{-3}y^2 \quad (1.1)$$

$$\%Recovery\frac{B}{C} = 12.27 + 4.68x + 1.47 \times 10^{-3}y - 0.29x^2 + 1.40 \times 10^{-2}xy - 0.61y^2 \quad (1.2)$$

$$\%Recovery\frac{A}{C} = -2.95 + 0.60x + 1.74 \times 10^{-2}y - 4.62 \times 10^{-3}x^2 - 8.75 \times 10^{-3}xy - 1.02y^2 \quad (1.3)$$

$$\%Recovery\frac{C}{D} = -2.70 + 1.07x + 2.24y - 31.41x^2 - 28xy - 8.71 \times 10^{-3}y^2 \quad (1.4)$$

Solution pH can greatly influence the adsorption of any analyte as it affects the surface charge of the adsorbent by distressing the protonation/deprotonation of the functional groups. To inspect the effects of pH on the extraction of the Pb(II), several pH solutions with same amount of CdZnS/ZnS@2-MAA (0.01 g) and same concentration of Pb(II) (100 ppb, 100 mL) were prepared. The pH was controlled with the backing of 1 M HCl and NaOH solution.

No removal of Pb(II) from water sample in strong acidic medium (pH < 2) was observed by the CdZnS/ZnS@2-MAA because the surface charge become positive which result in electrostatic repulsion between Pb(II) and adsorbent. Zero charge pH ($pH_{pzc}$) is the pH value where the surface charge of the sorbent is zero, at this pH the surface functionalities

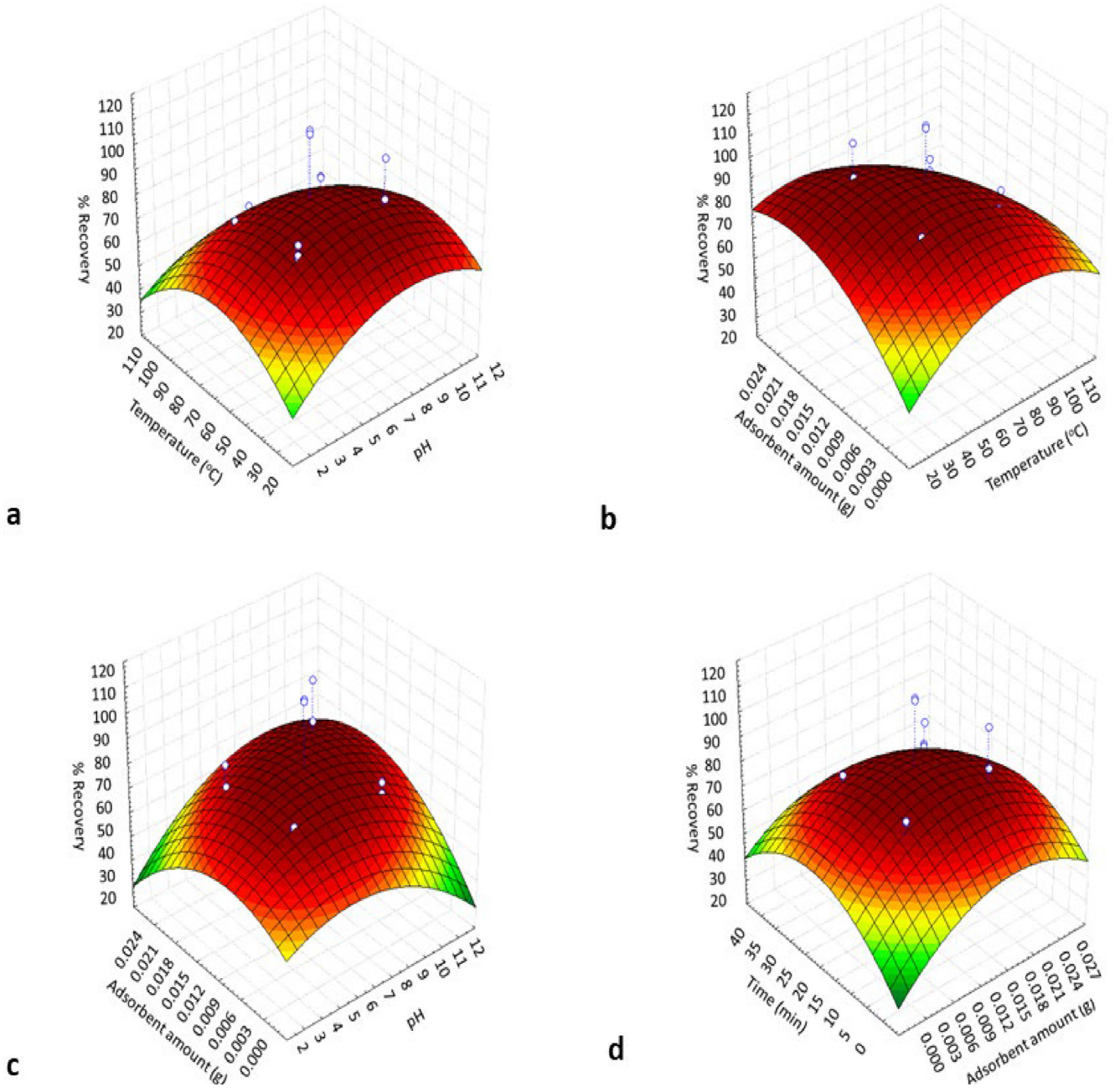


**Fig. 5** 3D Surface plot for the effect of significant variables on % recovery of analyte (n = 6); (a) pH vs temperature, (b) temperature vs adsorbent amount, (c) pH vs adsorbent amount, (d) adsorbent amount vs time.

(both acidic and basic) do not contribute to the overall pH value of the solution (Anari-Anaraki and Nezamzadeh-Ejhieh, 2015). Due to protonation and decline in the stability of metallic complex, lower adsorption of Pb(II) was observed at pH 4.0. The sorbent surface has a positive charge at pH lower than its $pH_{pzc}$, the reason is adsorption of $H^+$, thus avoiding the positive charged Pb(II) (Nezamzadeh-Ejhieh and Zabihi-Mobarakeh 2014). The Fig. 5a, shows maximum recovery can be obtained at pH 6.9. Equations (1.1) & (1.2) also confirmed the same pH value.

Since, temperature plays notable role in the extraction of an analyte, thus seven standard sample solutions having CdZnS/ZnS@2-MAA (0.01 g) and Pb(II) (100 ppb) were taken in separate beakers having thermometer with the temperature discreteness of 10 °C. The solutions were heated on the hotplate till temperature reached to require level with constant stirring. The adsorption of Pb(II) was secured at temperature 30 °C and further raised in temperature displayed the decreased in adsorption capacity. Three-dimensional surface diagrams (Fig. 5a-b, and Eqs. (1.1) & (1.2)) revealed that 61.1 °C temperature has the ability to yield 100 % recovery, so this amount was selected as optimum value.

Electrostatic adsorption, coordination adsorption and ion-exchange are primarily incorporated as the adsorptive modes for expulsion of metal ions (Yu et al., 2017). The electrostatic attraction in the adsorption process of Pb(II) with CdZnS/

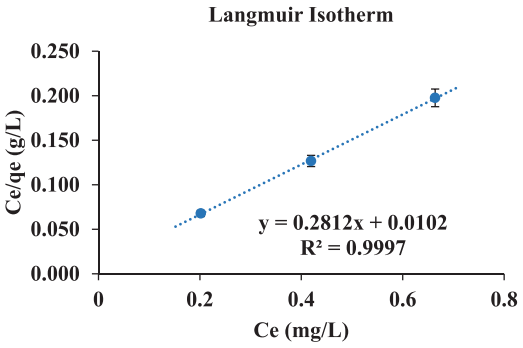


**Fig. 6** Langmuir adsorption isotherm.

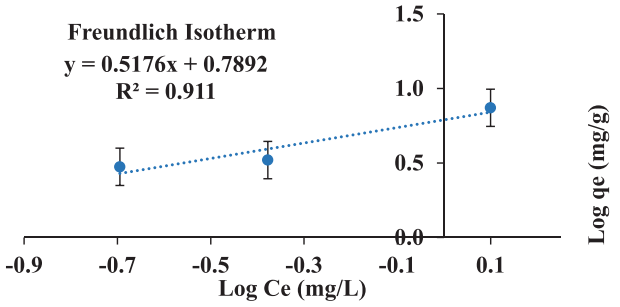


**Fig. 7** Freundlich adsorption isotherm.

ZnS@ 2-MAA was studied by preparing four standard sample solutions in a 200 mL glass beakers marked as beaker-I, beaker-II, beaker-III and beaker-IV having 100 ppb of Pb(II) in 100 mL de-ionize water and different amount of CdZnS/ZnS@ 2-MAA *i.e.*, as 0.005 g in beaker-I, 0.01 g in beaker-II, 0.015 g in beaker-III and 0.02 g in beaker-IV. It was observed that the Pb(II) adsorption increased promptly when the amount of QDs was increased (0.005–0.01 g). However, decrease in Pb(II) adsorption was noticed when more adsorbent was added (0.01–0.015 g). To calculate the maximum adsorption/desorption time of Pb(II) on CdZnS/ZnS@2-MAA, five standard solutions of Pb(II) in the deionized water were made. The time of standard and sample solutions was synchronized to 5.0 min. Furthermore, the Pb(II) extraction boosted when incubation time increased from 5 to 15 min which start to decline as time passes. The calculation from Eq. (1.3 & 1.4) indicated that the recoveries were quantitative at amount of adsorbent 0.013 g with 15.3 min of time for adsorption and desorption (Fig. 5c-d).

### *3.3. Adsorption isotherms*

The removal of Pb(II) from water using CdZnS/ZnS@2-MAA QDs on the AAS was studied under experimental parameters such as pH, time, temperature, adsorbent mass, and amount of Pb(II) for optimization. Langmuir adsorption model was applied with linear form of Langmuir's equation to predict the adsorption of analyte at definite localized homogenous sites of adsorbent (Lagergren, 1898).

$$\frac{C_e}{q_e} = \frac{1}{Q_m K_L} + \frac{C_e}{Q_m} \tag{2}$$

where, $q_e$ is (Pb(II)) amount per unit mass of QDs, $C_e$ is the equilibrium concentration of Pb(II) in aqueous solution (mg/L), $Q_m$ is the monolayer capacity (mg/g) and $K_L$ is binding constant. Graph was plotted between $C_e/q_e$ and $C_e$ as shown in Fig. 6. The results of $Q_m$ and $K_L$ values suggested a very weak interaction between the species (Table 3). The $R_L$ value (dimensionless) from the equation (3) was used to anticipate the nature of the adsorption process.

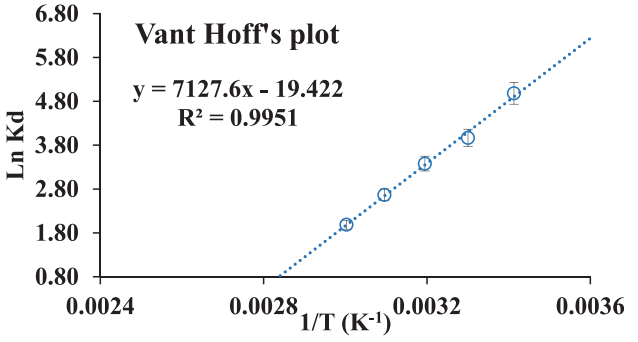


**Fig. 8** Van't Hoff plot.

$$R_L = \frac{1}{1 + (K_L C_o)} \tag{3}$$

where, $C_o$ is Pb(II) initial concentration in an aqueous solution and $K_L$ is Langmuir binding constant. The $R_L$ values equal to one in this study indicate that adsorption characteristic is linear (Aly et al., 2014).

Alternatively, Freundlich adsorption isotherm predicted the occurrence of adsorption on a heterogeneous surface with stronger binding sites occupied first (Naghash and Nezamzadeh-Ejhieh 2015). The adsorption model was applied by using linear form of Freundlich equation (Freundlich, 1907).

$$\log q_e = \log K_f + \frac{1}{n} \log C_e \tag{4}$$

where, $K_f$ and $n$ are Freundlich constants which represent the relative indicator of adsorption capacity and intensity of

**Table 3** Adsorption isotherm parameters for the adsorption of Pb(II) on quantum dot.

| Temperature | Langmuir Isotherm | | $R_L$ | Freundlich Isotherm | |
|---|---|---|---|---|---|
| 28 ± 2 °C | $Q_m$ | $K_L$ | | n | $K_F$ |
| | 3.56 | 0.003 | 1.00 | 1.92 | 6.1 |

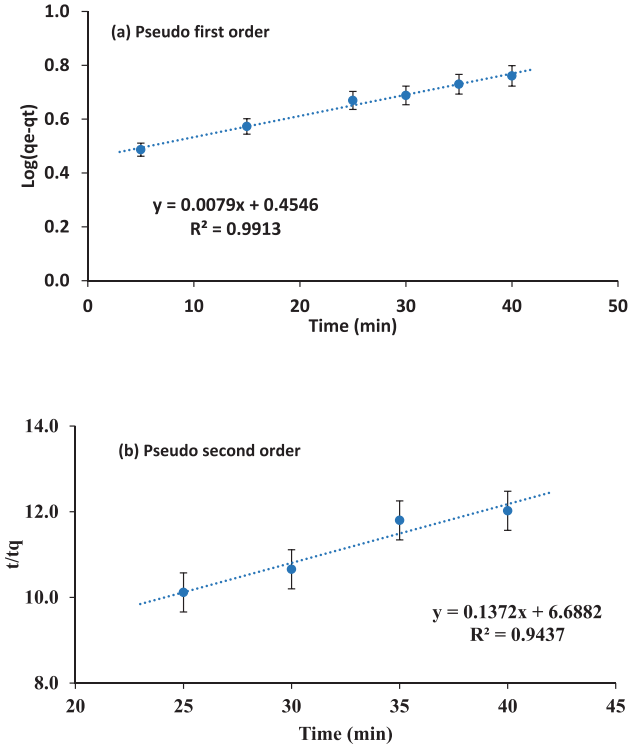


**Fig. 9** (a) Pseudo-first order (b) Pseudo-second order.

**Table 4** Thermodynamic parameters for the adsorption of Pb (II) on quantum dot.

| Temperature (°C) | LnKd | $\Delta G^{\circ}$ (KJ/molK) | $\Delta H^{\circ}$ (KJ/molK) |
|---|---|---|---|
| 30 | 3.97 | −9.99 | −59.26 |
| 40 | 3.38 | −8.80 | **$\Delta S^{\circ}$ (KJ/molK)** |
| 50 | 2.67 | −7.16 | |
| 60 | 1.99 | −5.50 | −0.16 |

adsorption. The graph was plotted between $\log q_e$ and $\log C_e$ (Fig. 7). Adsorption is favorable if the value of *n* is in the range $1 < n < 10$. In this case the value of *n* is 1.92 which indicates that Pb(II) adsorption was favorable and heterogeneous surface of QDs have larger adsorption capacity (Table 3). The obtained results indicated that Freundlich isotherms showed a good correlation coefficients ratio to Langmuir isotherms. This demonstrates that some Pb(II) species may get trapped between the organic chains of QDs double layers in addition to being removed by surface interaction.

### 3.4. Thermodynamic parameter

The thermodynamic studies were conducted between 20 and 100 °C. Thermodynamic factors such as entropy ($\Delta S^{\circ}$), enthalpy ($\Delta H^{\circ}$), and Gibb's free energy ($\Delta G^{\circ}$) are useful to define the nature of the adsorption. Therefore, Van't Hoff reaction isotherm was used to examine these parameters (al Sadat Shafiof and Nezamzadeh-Ejhieh, 2020).

$$\Delta G^{o} = -RTlnK_d \tag{5}$$

$$lnK_d = \left(\frac{\Delta S}{R}\right) - \left(\frac{\Delta H}{RT}\right) \tag{6}$$

where, $K_d$ = C/Ce is constant of equilibrium, C (mg/L) is the adsorbent concentration while Ce (mg/L) is the concentration of adsorbate at equilibrium condition. R is the gas constant (8.314 J $mol^{-1}$ $K^{-1}$) and T is the temperature in Kelvin. Graph was plotted between $\ln K_d$ and 1/T (Fig. 8).

The negative free energy confirms that the complex formation in between CdZnS/ZnS@2-MAA and Pb(II) is temperature dependent spontaneous process. These findings also indicated that the sorption is temperature sensitive since **ΔG** becomes less negative at elevated temperature (Nezamzadeh-Ejhieh and Kabiri-Samani, 2013). During complex formation the binding reaction was drive by negative enthalpy (−59.26 KJ/molK) which suggested that during adsorption exothermic reaction might have happened. While, negative enthalpy also means breakage of Pb(II)–$H_2O$ bond in aqueous medium is favorable for the formation of the pb(II)-QDs complex. Whereas negative entropy (−0.16 KJ/molK) suggests that complex formation contributes to decrease in randomness at internal structure of the adsorbent during adsorption with low amount of ion replacement. Thus complex formation due to the chemisorptions remains dominant process in Pb (II) removal (Table 4). Similar mechanisms were also reported for the CIZS-QDs and $Ag_2S$-QDs for the adsorption of Pb(II) and Cu(II) from aqueous mediums (Jiang et al., 2019; Han et al., 2022).

### 3.5. Kinetics of adsorption

The pseudo-first order model is useful for the systems where driving force model is linear and adsorption rate is associated to alteration in the saturated concentration and number of active adsorbent sites, indicating that the whole adsorption rate is proportional to the preliminary strength of process. The pseudo-second order model, instead suggests that the speed of mechanism is controlled by chemical adsorption, where universal adsorption rate is square of the preliminary strength of process and in it the molecules join the adsorbent surface (Khan et al., 2019). Therefore, adsorption process of Pb(II) on QDs was investigated by using these two kinetic models. The equations used for Lagergren's Pseudo first order and Ho Pseudo second order kinetics (Ho et al., 1999) are written as eq. (7) and eq.8. For first order modeling, graph was plotted between log (qe-qt) and t. While, for second order modeling graph was plotted between $t/q_t$ and t.

$$\log(q_e - q_t) = \log q_e - \frac{K_1}{2.303}t \tag{7}$$

$$\frac{t}{q_t} = \frac{1}{q_e^2 K_2} + \frac{1}{q_e}t \tag{8}$$

where, $q_e$ is the quantity of Pb(II) adsorbed on the QDs (mg/g) at equilibrium, qt is the mass of Pb(II) adsorbed on the QDS (mg/g) at time t, $K_1$ and $K_2$ are the rate constants of first and second order and t is the time in minute, Fig. 9 a-b. For both model straight line plots were obtained but equilibrium adsorption capacities ($q_e$) was better fitted with pseudo second order. These finding suggest that rate limiting steps involve exchange or sharing of electrons and/or chelation between the adsorbate and adsorbent by formation of chemi-sorptive

**Table 5** Pseudo-first order and pseudo-second order rate constants for the adsorption of Pb(II) on QDs.

| Temperature °C | Pseudo first order | | Pseudo second order | | $q_e$ (exp) |
|---|---|---|---|---|---|
| | $K_1$ | $q_e$ | $K_2$ | $q_e$ | |
| 28 ± 2 | −0.0182 | 2.8484 | 7.94 | 7.29 | 8.48 |

**Table 6** Applications of adsorbent on water samples for detection of Pb(II).

| Samples Origin | Added Pb ($ngmL^{-1}$) | Extracted Pb ($ngmL^{-1}$) | %Recovery | %RSD |
|---|---|---|---|---|
| Tap Water of Gulshan-e-Iqbal | 0 | 0.964 ± 0.015 | 96.4 | 1.55 |
| Campus FUUAST, Karachi City | 10 | 9.89 ± 0.13 | 98.9 | 1.31 |
| Ground water of Malir Cantt, | 0 | 0.948 ± 0.020 | 94.8 | 2.11 |
| Karachi City | 10 | 9.93 ± 0.69 | 99.3 | 6.95 |

*Recovery (%) = (Extracted / Added) × 100; RSD (%) = (SD/Mean) × 100.

**Table 7** Comparison of analytical methods for detection of Pb(II).

| QDs | LOD | Mode of detection | Ref |
|---|---|---|---|
| CdTe and CdZnSe QDs QDs capped with Glutathione | 20 nM | Fluorescence quench | (Mohamed Ali et al., 2007) |
| CdTe-QDs capped with cysteamine | 30 ppb | Fluorescence quench | (Wang and Guo, 2009) |
| CdS-QDs capped with pomegranate peel extract | $10^{-9}$ M | Naked eye detection | (Kaviya, 2018) |
| AgInS2-QDs capped with glutathione | 4 nM | Fluorescence quench | (Xue et al., 2021) |
| Graphene QDs capped with Dithienopyrrole derivative | 0.25 nM | Fluorescence quench | (Sebastian et al., 2021) |
| ZnSeS/Cu:ZnS/ZnS-QDs capped with 3-mercaptopropionic acid | 21 nM | Photoluminescent | (Mabrouk et al., 2022) |
| *Aspergillus sp* biosynthesized ZnS-QDs | 2.45 µM | Fluorescence quench | (Jacob et al., 2020) |
| CuInZnS-QDs capped with glutathione | $5.18 \times 10^{-7}$ M | Fluorescence quench | (Han et al., 2022) |
| CdZnS/ZnS QDs capped with 2-MAA | 0.1 ng/mL | Chemisorption | **This work** |

bond which could be influenced by intraparticle/pore diffusion through which the adsorbate ions might have entered in the interior pore positions of adsorbent (Table 5).

### 3.6. Pb(II) adsorption in water samples

The detection and recovery of Pb(II) in tap and ground water; samples were collected from FUUAST Gulshan-e-Iqbal Campus, Karachi and Malir Cantt (Karachi) and studied under optimized conditions i.e., 0.01 g CdZnS/ZnS@2-MAA dispersed in100 mL of water sample having pH 4.0 stirred for 20 min at 30 °C. Initially unknown concentration of Pb(II) in real water samples were detected in tap water (0.964 $ng.mL^{-1}$ with 96.4 % recovery) and ground water (0.948 $ngmL^{-1}$ with 94.8 % recovery) with small %RSD values 1.55 and 2.11, respectively. In second step 10 $ng.mL^{-1}$ of Pb(II) was added in both water samples. The result demonstrated that CdZnS/ZnS@2-MAA were able to remove 98.9 % Pb(II) from tap water samples with %RSD 1.31. While, 99.3 % Pb(II) was removed from ground water samples with 6.95 % of RSD (Table 6). Moreover, limit of detection and quantification (LOD and LOQ) of the CdZnS/ZnS@2-MAA QDs was also determined. The developed experimental process showed good conformity due to the low LOD (0.1 ng $mL^{-1}$) and LOQ (0.90 ng $mL^{-1}$) in comparison of reported QDs utilized for Pb(II) removal from aqueous medium (Table 7) and maximum permissible limit set by WHO for Pb(II) in drinking water (10 µg/L) (Naushad, 2014).

### 3.7. Regeneration analyses of CdZnS/ZnS-2-MAA QDs

The high adsorption capacity, effortless separation with low outlay and regeneration makes nano adsorbent convenient economically and technologically (Sari et al., 2007). In this research CdZnS/ZnS-2-MAA QDs were recycled with 99 % ethanol solution for further used. Moreover, recovered QDs have validated their functionality equal to the pure QDs when extraction of Pb(II) from solution was repeated.

### 3.8. Removal mechanism of Pb(II) by CdZnS/ZnS@2-MAA QDs

In CdZnS/ZnS@2-MAA, 2-MAA was utilized as capping agent which functions as stabilizing agent and brings electrostatic attraction between ZnS (shell) and Pb(II) in water samples. Overall Pb(II)adsorption is found to be favorable on the

QDs heterogeneous surface as Freundlich models predicted. The findings indicated that sorption is temperature sensitive since **ΔG** becomes less negative at elevated temperature. The negative **ΔG** also means that binding energy of QDs is stronger than Pb-solvent and this difference in energetic potentials of the system's components is what drives the redistribution of Pb(II) in the system and spontaneous sorption on QDs. Additionally, negative **ΔH** and **ΔS** showed that sorption is an exothermic process and complex formation-induced chemisorption as the primary mechanism for Pb(II) removal. The system follows the pseudo-second order rates in which rate-limiting step is a chemical reaction that was impacted by Pb(II) ion intraparticle/pore diffusion with QDs.

## 4. Conclusions

CdZnS/ZnS@2-MAA QDs were utilized as an adsorbent in a method for removing Pb(II) from water samples. The integration of numerous analytical approaches enabled the investigation of the kinetics, equilibrium, and mechanics of adsorption. The findings of this research are critical for enhancing the quality of the approach and in creating technological goals for the heavy metal ions removal procedures. The proposed technology is shown to be simple, inexpensive, accurate, and non-destructive which makes it a feasible option for other systems that demand more resources and effort.

## Declaration of Competing Interest

The authors declare that they have no known competing financial interests or personal relationships that could have appeared to influence the work reported in this paper.

## Appendix A. Supplementary material

Supplementary data to this article can be found online at https://doi.org/10.1016/j.arabjc.2022.104224.

## References


al Sadat Shafiof, M., Nezamzadeh-Ejhieh, A., 2020. A comprehensive study on the removal of Cd (II) from aqueous solution on a novel pentetic acid-clinoptilolite nanoparticles adsorbent: Experimental design, kinetic and thermodynamic aspects. Solid State Sci. 99, 106071.

Alivisatos, A.P., 1996. Perspectives on the physical chemistry of semiconductor nanocrystals. J. Phys. Chem. 100, 13226–13239.

Aly, Z., Graulet, A., Scales, N., et al, 2014. Removal of aluminium from aqueous solutions using PAN-based adsorbents: characterisation, kinetics, equilibrium and thermodynamic studies. Environ. Sci. Pollut. Res. 21, 3972–3986.

Amarasinghe, B., Williams, R.A., 2007. Tea waste as a low cost adsorbent for the removal of Cu and Pb from wastewater. Chem. Eng. J. 132, 299–309.

Anari-Anaraki, M., Nezamzadeh-Ejhieh, A., 2015a. Modification of an Iranian clinoptilolite nano-particles by hexadecyltrimethyl ammonium cationic surfactant and dithizone for removal of Pb (II) from aqueous solution. J. Colloid Interface Sci. 440, 272–281.

Anari-Anaraki, M., Nezamzadeh-Ejhieh, A., 2015b. Modification of clinoptilolite nanoparticles by a cationic surfactant and dithizone for removal of Pb (II) from aqueous solution. J. Colloid Interface Sci. 440, 272–281.

Chan, W.C., Maxwell, D.J., Gao, X., et al, 2002. Luminescent quantum dots for multiplexed biological detection and imaging. Curr. Opin. Biotechnol. 13, 40–46.

Chen, Q., Yao, Y., Li, X., et al, 2018. Comparison of heavy metal removals from aqueous solutions by chemical precipitation and characteristics of precipitates. J. Water Process Eng. 26, 289–300.

Costa-Fernandez, J.M., 2006. Optical sensors based on luminescent quantum dots. Anal. Bioanal. Chem. 384, 37–40.

Dilshad, A., Anwer, H., Shah, F., et al, 2021. Biosorptive Removal of Cr (VI) from Aqueous Solution by Araucaria Cunninghamii Linn: A Multivariate Study. Anal. Lett. 54, 1243–1268.

Franke, D., Harris, D.K., Chen, O., et al, 2016. Continuous injection synthesis of indium arsenide quantum dots emissive in the short-wavelength infrared. Nat. Commun. 7, 1–9.

Freundlich, H., 1907. Über die adsorption in lösungen. Z. Phys. Chem. 57, 385–470.

Gurreri, L., Cipollina, A., Tamburini, A., et al, 2020. Electrodialysis for wastewater treatment—Part II: Industrial effluents. Current Trends and Future Developments on (Bio-) Membranes. r, 195–241.

Han, X., Yu, F., Lei, J., et al, 2022. Pb2+ Responsive Cu-In-Zn-S Quantum Dots With Low Cytotoxicity. Front. Chem. 10.

Hargreaves, A.J., Vale, P., Whelan, J., et al, 2018a. Coagulation–flocculation process with metal salts, synthetic polymers and biopolymers for the removal of trace metals (Cu, Pb, Ni, Zn) from municipal wastewater. Clean Technol. Environ. Policy 20, 393–402.

Hargreaves, A.J., Vale, P., Whelan, J., et al, 2018b. Impacts of coagulation-flocculation treatment on the size distribution and bioavailability of trace metals (Cu, Pb, Ni, Zn) in municipal wastewater. Water Res. 128, 120–128.

Heidari-Chaleshtori, M., Nezamzadeh-Ejhieh, A., 2015. Clinoptilolite nano-particles modified with aspartic acid for removal of Cu (II) from aqueous solutions: isotherms and kinetic aspects. New J. Chem. 39, 9396–9406.

Ho, Y., Yu, L., Liu, H., 1999. Rotor dynamic coefficients of a thrust active magnetic bearing considering runner tilt. Proc. Inst. Mech. Eng., Part J: J. Eng. Tribol. 213, 451–462.

Jacob, J.M., Rajan, R., Kurup, G.G., 2020. Biologically synthesized ZnS quantum dots as fluorescent probes for lead (II) sensing. Luminescence 35, 1328–1337.

Jiang, P., Li, S., Han, M., et al, 2019. Biocompatible Ag 2 S quantum dots for highly sensitive detection of copper ions. Analyst. 144, 2604–2610.

Jiang, M.-Q., Wang, Q.-P., Jin, X.-Y., et al, 2009. Removal of Pb (II) from aqueous solution using modified and unmodified kaolinite clay. J. Hazard. Mater. 170, 332–339.

Kaviya, S., 2018. Size dependent ratiometric detection of Pb (II) ions in aqueous solution by light emitting biogenic CdS NPs. J. Lumin. 195, 209–215.

Kazemifard, N., Ensafi, A.A., Dehkordi, Z.S., 2021. A review of the incorporation of QDs and imprinting technology in optical sensors–imprinting methods and sensing responses. New J. Chem. 45, 10170–10198.

Khan, I., Saeed, K., Khan, I., 2019. Nanoparticles: Properties, applications and toxicities. Arabian J. Chem. 12, 908–931.

Kumari, L., Kar, A.K., 2020. Compositional variation dependent colour tuning and observation of Förster resonant energy transfer in Cd (1–x) Zn x S nanomaterials. New J. Chem. 44, 870–883.

Lagergren, S.K., 1898. About the theory of so-called adsorption of soluble substances. Sven. Vetenskapsakad. Handingarl. 24, 1–39.

Liu, X., Jiang, Y., Fu, F., et al, 2013. Facile synthesis of high-quality ZnS, CdS, CdZnS, and CdZnS/ZnS core/shell quantum dots: characterization and diffusion mechanism. Mater. Sci. Semicond. Process. 16, 1723–1729.

Ma, Y., Mao, G., Huang, W., et al, 2019. Quantum dot nanobeacons for single RNA labeling and imaging. J. Am. Chem. Soc. 141, 13454–13458.

Mabrouk, S., Rinnert, H., Balan, L., et al, 2022. Aqueous synthesis of core/shell/shell ZnSeS/Cu: ZnS/ZnS quantum dots and their use as a probe for the selective photoluminescent detection of Pb2+ in water. J. Photochem. Photobiol., A 114050.

Masab, M., Muhammad, H., Shah, F., et al, 2018. Facile synthesis of CdZnS QDs: Effects of different capping agents on the photoluminescence properties. Mater. Sci. Semicond. Process. 81, 113–117.

Mohamed Ali, E., Zheng, Y., Yu, H.-H., et al, 2007. Ultrasensitive Pb2 + detection by glutathione-capped quantum dots. Anal. Chem. 79, 9452–9458.

Murray, A., Örmeci, B., 2019. Use of polymeric sub-micron ion-exchange resins for removal of lead, copper, zinc, and nickel from natural waters. J. Environ. Sci. 75, 247–254.

Naghash, A., Nezamzadeh-Ejhieh, A., 2015. Comparison of the efficiency of modified clinoptilolite with HDTMA and HDP surfactants for the removal of phosphate in aqueous solutions. J. Ind. Eng. Chem. 31, 185–191.

Naushad, M., 2014. Surfactant assisted nano-composite cation exchanger: development, characterization and applications for the removal of toxic Pb2+ from aqueous medium. Chem. Eng. J. 235, 100–108.

Nawaz, T., Zulfiqar, S., Sarwar, M.I., et al, 2020. Synthesis of diglycolic acid functionalized core-shell silica coated Fe3O4 nanomaterials for magnetic extraction of Pb (II) and Cr (VI) ions. Sci. Rep. 10, 1–13.

Nezamzadeh-Ejhieh, A., Kabiri-Samani, M., 2013. Effective removal of Ni (II) from aqueous solutions by modification of nano particles of clinoptilolite with dimethylglyoxime. J. Hazard. Mater. 260, 339–349.

Nezamzadeh-Ejhieh, A., Zabihi-Mobarakeh, H., 2014. Heterogeneous photodecolorization of mixture of methylene blue and bromophenol blue using CuO-nano-clinoptilolite. J. Ind. Eng. Chem. 20, 1421–1431.

Okereafor, U., Makhatha, M., Mekuto, L., et al, 2020. Toxic metal implications on agricultural soils, plants, animals, aquatic life and human health. Int. J. Environ. Res. Public Health 17, 2204.

Peng, X., Luan, Z., Di, Z., et al, 2005. Carbon nanotubes-iron oxides magnetic composites as adsorbent for removal of Pb (II) and Cu (II) from water. Carbon 43, 880–883.

Prasad, M., Xu, H.-Y., Saxena, S., 2008. Multi-component sorption of Pb (II), Cu (II) and Zn (II) onto low-cost mineral adsorbent. J. Hazard. Mater. 154, 221–229.

Reed, B.E., Vaughan, R., Jiang, L., 2000. As (III), As (V), Hg, and Pb removal by Fe-oxide impregnated activated carbon. J. Environ. Eng. 126, 869–873.

Sari, A., Tuzen, M., Citak, D., et al, 2007. Equilibrium, kinetic and thermodynamic studies of adsorption of Pb (II) from aqueous solution onto Turkish kaolinite clay. J. Hazard. Mater. 149, 283–291.

Sebastian, D., Kala, R., Neethu Parvathy, K., et al, 2021. A fluorescent probe based on visible light-emitting functionalized Graphene Quantum dots for the sensitive and selective detection of Pb (II) ions. J. Mater. Sci. 56, 18126–18146.

Staff, W. H. O. and W. H. Organization, 1996. Cancer pain relief: with a guide to opioid availability, World Health Organization.

Sultanbayeva, G.S., Holze, R., Chernyakova, R., et al, 2013. Removal of Fe2+-, Cu2+-, Al3+-and Pb2+-ions from phosphoric acid by sorption on carbonate-modified natural zeolite and its mixture with bentonite. Microporous Mesoporous Mater. 170, 173–180.

Thaçi, B.S., Gashi, S.T., 2019. Reverse osmosis removal of heavy metals from wastewater effluents using biowaste materials pretreatment. Pol. J. Environ. Stud. 28, 337–341.

Wang, X., Guo, X., 2009. Ultrasensitive Pb 2+ detection based on fluorescence resonance energy transfer (FRET) between quantum dots and gold nanoparticles. Analyst. 134, 1348–1354.

Wu, J., Wang, T., Wang, J., et al, 2021. A novel modified method for the efficient removal of Pb and Cd from wastewater by biochar: Enhanced the ion exchange and precipitation capacity. Sci. Total Environ. 754, 142150.

Xue, T., Shi, Y., Guo, J., et al, 2021. Preparation of AgInS2 quantum dots and their application for Pb2+ detection based on fluorescence quenching effect. Vacuum 193, 110514.

Yakoubi, A., Chaabane, T.B., Aboulaich, A., et al, 2016. Aqueous synthesis of Cu-doped CdZnS quantum dots with controlled and efficient photoluminescence. J. Lumin. 175, 193–202.

Yu, C., Shao, Z., Hou, H., 2017. A functionalized metal–organic framework decorated with O− groups showing excellent performance for lead (II) removal from aqueous solution. Chem. Sci. 8, 7611–7619.

Zhu, L., Ji, J., Wang, S., et al, 2018. Removal of Pb (II) from wastewater using Al2O3-NaA zeolite composite hollow fiber membranes synthesized from solid waste coal fly ash. Chemosphere 206, 278–284.

Zou, L., Gu, Z., Sun, M., 2015. Review of the application of quantum dots in the heavy-metal detection. Toxicol. Environ. Chem. 97, 477–490.